

**Title: CD206+ macrophages are relevant non-invasive imaging biomarkers and therapeutic targets in experimental lung fibrosis**

**Authors:** Lenny Pommerolle<sup>1,3#</sup>, Guillaume Beltramo<sup>1,2,3#</sup>, Léo Biziorek<sup>1,3</sup>, Marin Truchi<sup>4</sup>, Alexandre Magno Manesch Dias<sup>5</sup>, Julie Tanguy<sup>1,3</sup>, Lucile Dondaine<sup>1,3</sup>, Nicolas Pernet<sup>1,2,6</sup>, Victor Goncalves<sup>7</sup>, Alexanne Bouchard<sup>5</sup>, Marie Monerrat<sup>5</sup>, Grégoire Savary<sup>8</sup>, Nicolas Pottier<sup>8</sup>, Kjetil Ask<sup>9</sup>, Martin Kolb<sup>9</sup>, Bernard Mari<sup>4</sup>, Carmen Garrido<sup>1,2</sup>, Bertrand Collin<sup>5,7</sup>, Philippe Bonniaud<sup>1,2,3\*</sup>, Olivier Burgy<sup>1,2,3†</sup>, Françoise Goirand<sup>1,2,3†</sup>, Pierre-Simon Bellay<sup>1,3,5†</sup>.

**Affiliations:**

<sup>1</sup>INSERM U1231, Equipe HSP-pathies, Faculty of Medicine and Pharmacy, Dijon France.

<sup>2</sup>University of Bourgogne-Franche Comté, LIPSTIC, Dijon, France.

<sup>3</sup>Centre de Référence Constitutif des Maladies Pulmonaires Rares de l'Adultes de Dijon, réseau OrphaLung, Filière RespiFil, Centre Hospitalier Universitaire de Bourgogne, Dijon, France.

<sup>4</sup>Université Côte d'Azur, CNRS, Institut de Pharmacologie Moléculaire et Cellulaire, Sophia Antipolis, France.

<sup>5</sup>Centre George-François Leclerc, Service de médecine nucléaire, Plateforme d'imagerie et de radiothérapie précliniques, 1 rue du professeur Marion, Dijon, France.

<sup>6</sup>Plateforme de Cytométrie, Université de Bourgogne, Faculté de Médecine, 7 Bd Jeanne d'Arc 21000 Dijon, France.

<sup>7</sup>Institut de Chimie Moléculaire de l'Université de Bourgogne, UMR CNRS 6302, Université de Bourgogne Franche-Comté, 21000 Dijon, France.

<sup>8</sup>Université de Lille, CNRS, Inserm, CHU Lille, UMR9020 - UMR-S 1277, F-59000 Lille, France

<sup>9</sup>Department of Medicine, Firestone Institute for Respiratory Health, McMaster University, Hamilton, ON, Canada.

\*Corresponding author. Philippe Bonniaud, CHU Dijon, 14 Rue Paul Gaffarel, 21000 Dijon, +33 (0)3 80 29 37 72, philippe.bonniaud@chu-dijon.fr.

† These authors contributed equally to this work

# These authors contributed equally to this work

**Running title:** M2 macrophage: theranostic target in lung fibrosis

**Supplemental material****Detailed material and methods***Human tissue samples*

Lung tissue samples (n = 8) were obtained by open lung biopsy (FIRH, Hamilton, Canada).

Idiopathic pulmonary fibrosis (IPF) was diagnosed according to the American Thoracic Society/European Respiratory Society consensus criteria, including clinical, radiographic, and characteristic histopathologic features. Control non-IPF lung tissue samples were obtained from smokers who underwent thoracic surgery for localized primary lung carcinoma (biopsy away from cancer lesion, n= 8).

### *Radiolabelling*

Tilmanocept (Lymphoseek™, Navidea Biopharmaceuticals Europe Ltd, 62.5 µg) was reconstituted with 200 µl of 0.9% NaCl and added to a solution of <sup>99m</sup>Tc in a Lobind microtube (Eppendorf) in order to obtain 2350 ng of tilmanocept for 150 MBq per 1 ml. The microtube is then placed under agitation at 1000 rpm for 15 min at 25°C. The radiochemical purity was checked by radio-ITLC (Instant Thin Layer Chromatography) using a γ radiochromatograph (AR-2000 Radio-TLC & Imaging Scanner (Bioscan)). The stationary chromatography phase was a cellulose chromatographic paper (Whatman Grade 1, 3MM, 31ET Chr) where 1 µl of solution was deposited. The eluent used was acetone, it makes it possible to separate the free <sup>99m</sup>Tc from the <sup>99m</sup>Tc linked to tilmanocept. In this system, the <sup>99m</sup>Tc-tilmanocept remains at the deposition point while the radionuclide migrates to the solvent front. The radiochromatograph obtained gives the radiolabelling yield and the radiochemical purity by integration of the different peaks present. Results have been obtained using the software WinScan software.

### *Lung tissue dissociation*

Briefly, mice were anesthetized with a mix of ketamine (100 mg/kg) and xylazine (10 mg/kg) and euthanized by abdominal aortic bleeding. Cardiac lavage was performed with NaCl 0.9% before to harvest lung. Lung was cut and digested into collagenase (1.5 mg/ml, C0130, Sigma-Aldrich) and DNase I (0.1 mg/ml, 10104159001, Roche) solution in DMEM solution for 45 min at 37°C under agitation. Medium was collected and tissue were pounded in 70 µM filter to collect interstitial cells. The remaining red blood cells were lysed using homemade hemolytic

solution (NH<sub>4</sub>Cl 150 mM, KHCO<sub>3</sub> 10 mM, EDTA 0.1 mM). The resultant cells were counted by using trypan blue and 1 million cells were used for flow cytometry staining.

*Peripheral Blood Mononuclear Cells (PBMC)-derived macrophages isolation from healthy donors*

Buffy coats were obtained from Etablissement Français du Sang (EFS, Dijon, France) and PBMC separated using Ficoll density gradient. After adhesion, monocytes were cultivated in RPMI 10% FBS with 100 ng/ml M-CSF (130-096-492, Miltenyi Biotec, Germany) for 7 days. Then, cells were activated with IL-4 (130-093-922, Miltenyi Biotec) in presence of nintedanib (BIBF 1120, Selleckchem.com) or tofacitinib citrate (PZ0017, Sigma-Aldrich, Merck, France) for 48h. Tofacitinib were added to the culture 1h before IL-4 treatment and keep during all procedure. Cells were harvested by Accutase<sup>TM</sup> Cell Detachment solution (561527, BD Bioscience) before flow cytometry analysis.

*Conventional Flow cytometry analysis*

Both panel (PBMC and tissue lung cells) were analyzed on LSRFortessa flow cytometer (BD Biosciences, USA) using application settings in order to standardize cytometer between days. A minimum of 50,000 single events negative for FVS staining were recorded for each sample. Compensation values for spectral overlap were determined using BD<sup>TM</sup> Comp Beads anti-Rat and anti-Hamster Ig κ (552845, BD Bioscience) or BD<sup>TM</sup> Comp Beads anti-Mouse Ig κ (552843, BD Bioscience) depending on panel. A 2 µl suspension of both the positive and negative capture beads was singly stained with each fluorescent antibody as before. Post-acquisition analysis and

compensation was performed with FlowJo Version 10.7.2 (Treestar Inc, USA) software. Data analysis was performed using supervised method. The expression of selected markers was presented as Median Fluorescence Intensity (MFI). For gating control, Fluorescence Minus One (FMO) staining were used on cells where all antibodies except one were added to individual control tubes following the same protocol than antibodies staining.

#### *Unsupervised t-SNE analysis*

For lung tissue, an unsupervised t-distributed stochastic neighbor embedding (t-SNE) analysis was performed in FlowJo version 10.7.2 implementing R×64 Version 4.1.0. FCS files from each mouse was first cleaned using FlowAI plugin Version 2.3 (Monaco et al., 2016). Single live cells were then gated and exported to new FCS files. Prior to FlowSOM and FIt-SNE analyses, samples were subjected to random downsampling to 30,000 events using the DownSample plugin, Version 3.3.1 All files were finally concatenated together to generate a single expression matrix. FlowSOM analyses were performed using the FlowSOM plugin, version 3.0.16 (23), based on the 7 channels (Comp-CD45-A, Comp-CD11b-A, Comp-F4/80-A, Comp-Ly6g-A, Comp-SiglecF-A and Comp-CD206-A) with standard settings. The number of metaclusters was set to 10. The output generated a heat map showing each marker expression in all 10 clusters. t-SNE analyses were performed using the Fast Fourier Transform-accelerated Interpolation-based t-SNE (FIt-SNE) plugin, Version 0.5.1 (22), using the 7 channels as for FlowSOM, and with standard settings. The output generated two-dimensional dot (t-SNE dimension 1 and t-SNE dimension 2). Intensities for interest markers were overlaid with the dot-plot in order to facilitate assignment of cells subset. Clusters generated by FlowSUM were finally visualized on t-SNE plot.

### *Single cell RNA sequencing of BLM-treated mice*

Experimental design and animal treatment. All animal care and experimental protocols were conducted according to European, national and institutional regulations (Protocol numbers: 00236.03, IPMC agreement number E06152). Personnel from the laboratory performed all experimental protocols under strict guidelines to ensure careful and consistent handling of the mice. Seven-week (“young”) and 18-month (“old”)-old C57BL/6 male mice (Charles River) were divided randomly into two groups: (A) saline-only (PBS, n=3), or (B) bleomycin (Bleo, n=3). To induce fibrotic changes, 50- $\mu$ l bleomycin (1 U/kg) or PBS was aerosolized in mouse lungs using a MicroSprayer Aerosolizer (Penn-Century, Inc.) as previously described [1]. Mice were sacrificed at designated time points (days 14 and 28) after instillation. Lung single cell suspensions were generated as previously described [2]. Briefly, after euthanasia, lung tissue was perfused with sterile saline through the heart and were inflated through the trachea with dissociation cocktail containing dispase (50 caseinolytic U/ml), collagenase (2 mg/ml), elastase (1 mg/ml), and DNase (30  $\mu$ g/ml). Lungs were immediately removed, minced to small pieces (~1 mm<sup>3</sup>), and transferred for mild enzymatic digestion for 20–30 min at 37 °C in 4 ml of the dissociation cocktail. Enzymatic activity was inhibited by adding 5 ml of PBS supplemented with 10% fetal calf serum (FCS). Single cells suspensions were passed through a 40 micron mesh, and then collected after centrifugation at 300 g for 5 min (4°C). Red blood cell lysis was performed using RBC lysis buffer (Thermo fisher) for 2 minutes at 4°C and stopped using PBS 10% FCS. After another centrifugation at 300 g for 5 min (4°C) cells were counted and critically assessed for single cell separation and overall cell viability using the Countess 3 FL (Fisher Scientific). Samples were then stained for multiplexing using cell hashing [3], using the Cell

Hashing Total-Seq-ATM protocol (Biolegend) following the protocol provided by the supplier, using 6 distinct Hash Tag Oligonucleotides-conjugated mAbs (3 PBS and 3 Bleo). Samples were then adjusted to the same concentration and mixed in PBS supplemented with 0.04% of bovine serum albumin at a final concentration of 100 cells/ $\mu$ l. Single-cell capture was performed using the 10X Genomics Chromium device (3' V3). Single-cell libraries were sequenced on the Illumina NextSeq 500. Alignment of reads from the single cell RNA-seq library and unique molecular identifiers (UMIs) counting were performed with 10X Genomics Cell Ranger tool (v3.0.2). Reads of oligonucleotides tags (HTOs) used for Cell Hashing were counted with CITE-seq-Count [3] (v1.4.2). All downstream analyses were carried out with Seurat [4] R package (v4.1.0). For each sequencing run, UMIs and HTOs counts were integrated into a Seurat object. HTOs counts were demultiplexed with HTODemux function to assign sample-of-origin for each cell. Only the cells identified as "Singlet" and passing quality control metrics (UMIs and mitochondrial content arbitrary thresholds) were kept. Cells were regrouped into "samples" Seurat objects, according to treatment (PBS or BLM), age (young or old) and time of sacrifice (D14 or D28) combination, then normalized with SCTransform function. Preliminary to integration, the top 3000 variable features of each object were identified as anchors and used to compute principal component analysis (PCA). A set of common anchors were found in dimensionally reduced data using FindIntegrationAnchors function with the following arguments: `dims = 1:50`, `reduction = "rpca"`, `k.anchor = 5`; and then used for the dataset integration. PCA, UMAP and kNN Clustering were computed on the first 80 principal components (PCs) of the integrated data slot. Clusters were annotated using canonical markers of Endothelial, Mesenchymal, Epithelial and Immune populations. Macrophages were extracted and subclustered using the same precomputed 80 PCs. UMAP was rerun on this subset. The original

raw counts were finally log-normalized with NormalizeData for data exploration. Macrophages subpopulations were annotated according to their most differentially expressed genes described in Joshi *et al* [5].

### *Immunofluorescence*

After deparaffination (Xylene) and antigen unmasking (30 min in citrate buffer pH 6), sections from human biopsies from control or IPF patients as well as mice receiving NaCl or BLM were saturated (BSA 8%) and incubated overnight at 4°C with specific antibodies at a dilution of 1:100 for the detection of collagen (thermofischer scientific, USA), CD206 (Abcam, France) and CD68 (thermofischer scientific). Alexa488-, Alexa568- and Alexa 647-conjugated secondary antibodies (Abcam) were used (1:250, 45 min). Slides were mounted in Prolong-gold with DAPI (ProLong® Gold antifade reagent with DAPI, Life technologies).

## Supplemental figures

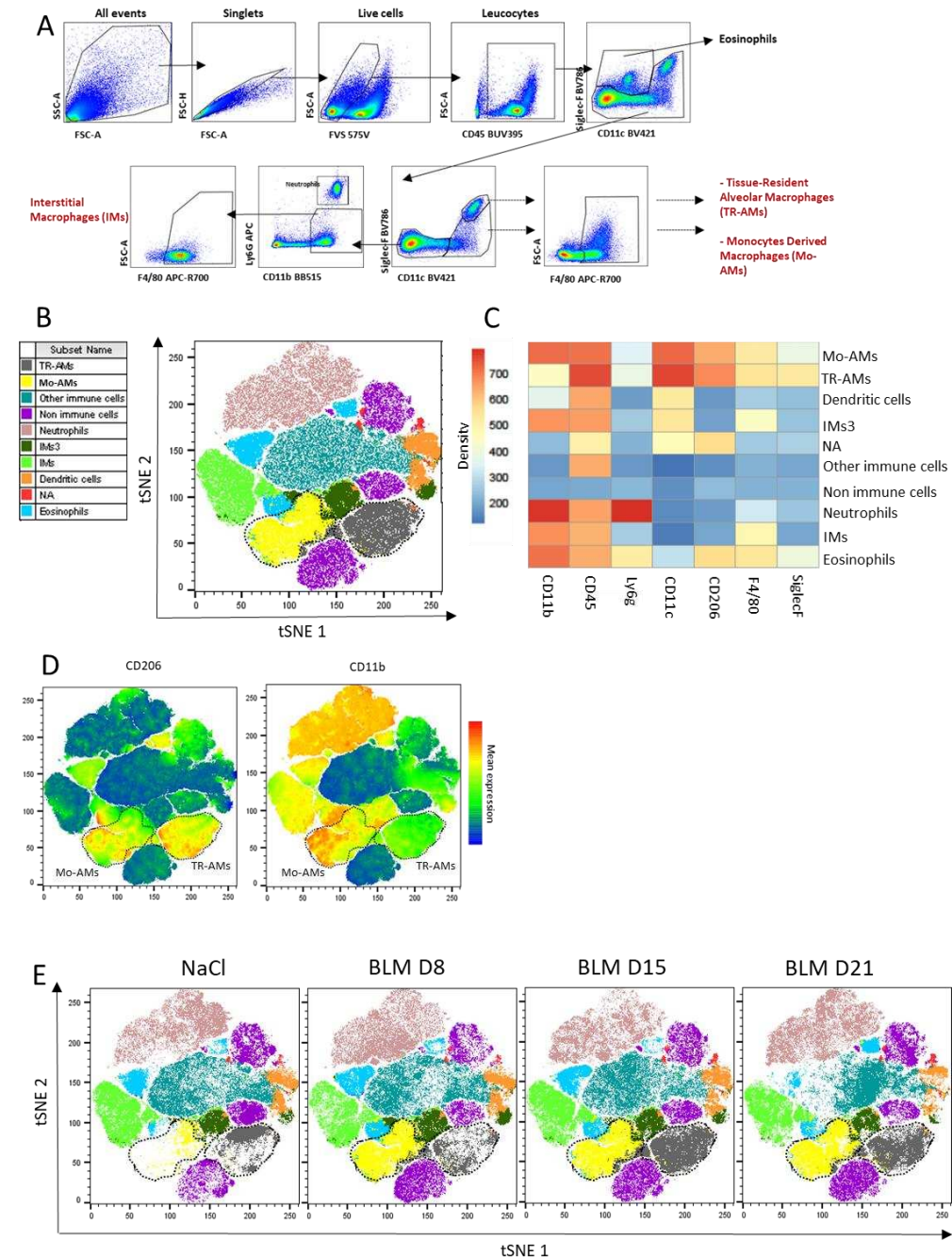


**Fig. S1 Macrophage profiling by flow cytometry in BLM-induced lung fibrosis**

A/ Gating strategy for Tissue-Resident Alveolar Macrophages (TR-AMs), Recruited-Monocytes Derived Macrophages (Mo-AMs) and Interstitial Macrophages (IMs) in flow cytometry. First gates were realized to eliminate debris (SSC-A/FSC-A), doublet cells (FSC-H/FSC-A). Live cells



were gated by the absence of FVS staining and leucocytes were selected by CD45 staining. Then, eosinophils were excluded from CD45 cells (CD11cdim, SiglecF+) to avoid their PE autofluorescence. The remainder of cells were used to determine all the other gates. SiglecF+, CD11c+ cells allowed us to get TR-AMs and SiglecFdim, CD11cdim/+ to get Mo-AMs. Double negative were then gated on Ly6-g to exclude neutrophils and Ly6g-, Cd11b+ allowed us to get IMs. TR-AMs, Mo-AMs and IMs were checked with F4/80 staining before MFI and percentage analysis. (B) Representative tSNE dimension 1 and 2 density plots of the lung subpopulations determined thanks to heat map (C) after intra-tracheal injection of bleomycin (BLM, 2mg/kg) or NaCl. The four groups of mice (NaCl, BLM sacrificed at day 8, 15 and 21) were concatenated for this tSNE analysis. B/ Representative tSNE dimension 1 and 2 density plots of lung CD206 expression (left) and CD11b expression (right) in concatenated groups. E/ Representative tSNE dimension 1 and 2 plots the lung subpopulations. Mice belonging to the same group were concatenated together in order to follow the evolution of each population for each time point. To note, the apparent expression of CD206 by eosinophils represented an artefact due to their autofluorescence in the phycoerythrin (PE) channel as previously described [6].

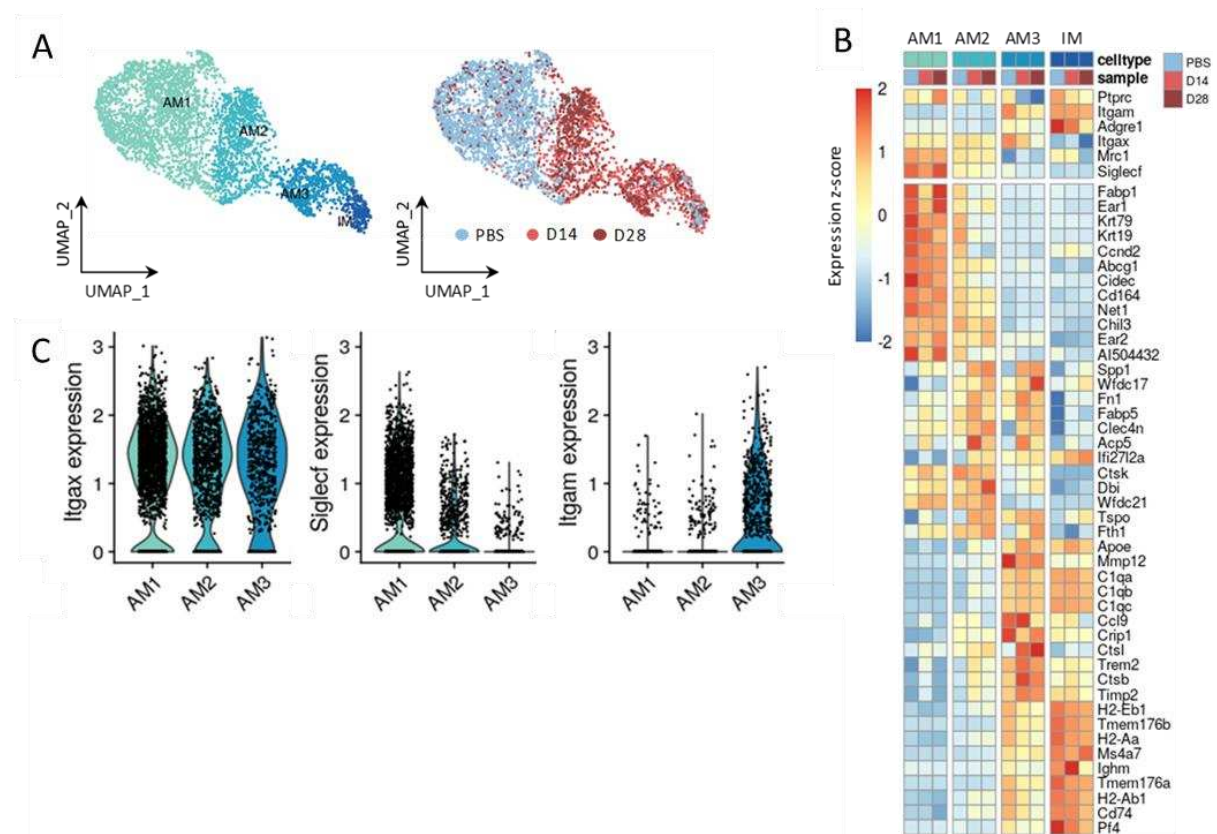


**Fig. S2 Macrophage profiling by scRNAseq in BLM-induced lung fibrosis**

A/ UMAP representation of scRNA-seq data corresponding to macrophages subpopulations extracted from the analysis of whole mice lungs collected 14 or 28 days after injection of PBS or bleomycin. AM = alveolar macrophages; IM = interstitial macrophages. B/ Heatmap of genes

coding for flow cytometry markers (top) and macrophages subpopulations markers identified by scRNA-seq analyses. C/ Normalized expression of genes coding for *Itgax*, *Siglecf* and *Itgam* in the alveolar macrophage subpopulations.

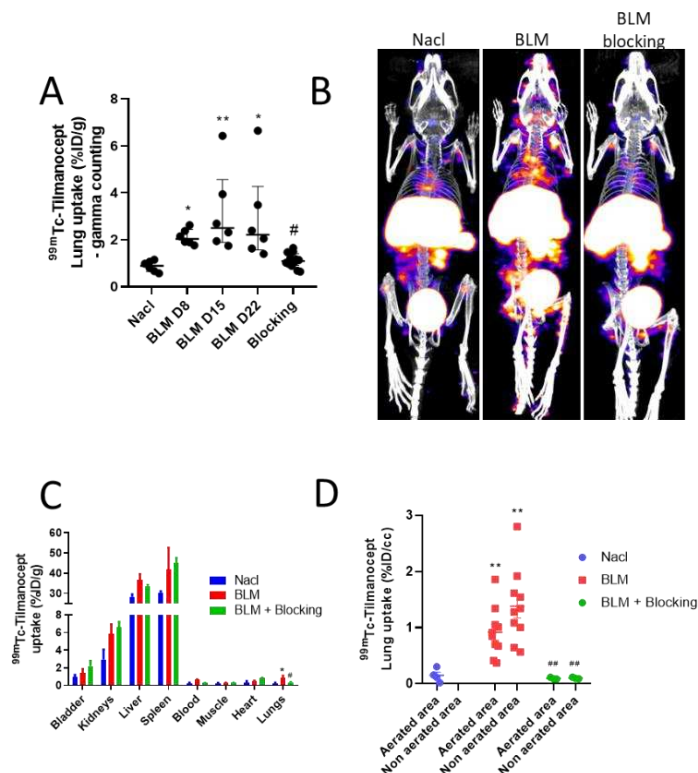


**Fig. S3** <sup>99m</sup>Tc-tilmanocept is able to detect advanced BLM-induced lung fibrosis.

A/ Graph represents the <sup>99m</sup>Tc-tilmanocept lung uptake in %ID/g measured by gamma counting of NaCl- and BLM-receiving mice at D8, D15 and D22. Results are presented as median  $\pm$  interquartile range, n = 6 for all groups. Stars (\*) are representative of comparison of each group with NaCl group and hashes (#) are representative of statistical comparison of blocking group with BLM D22 group. Difference between groups were compared using Kruskal-Wallis non-parametric ANOVA. \*p<0.05, \*\*\*p<0.001. B/ Representative Maximum intensity projection (MIP) image of <sup>99m</sup>Tc-tilmanocept (and blocking) whole body uptake of NaCl- and BLM-receiving mice. C/ <sup>99m</sup>Tc-tilmanocept uptake (%ID/g) in bladder, kidneys, liver, spleen, blood, muscle, heart and lungs in NaCl- and BLM-receiving mice. Stars (\*) are representative of comparison of each group with NaCl group and hashes (#) are representative of statistical comparison of blocking group with BLM group. Difference between groups were compared using Kruskal-Wallis non-parametric ANOVA. \*p<0.05. D/ Graph represents the <sup>99m</sup>Tc-tilmanocept lung uptake in %ID/cc of NaCl- and BLM-receiving mice at D22 in aerated and non-aerated lung areas (segmented on CT images). Results are presented as median  $\pm$  interquartile range, NaCl n=4, BLM n=10, BLM + blocking = 3. Difference between groups were compared using Kruskal-Wallis non-parametric ANOVA, \*\*(#)#p<0.01.

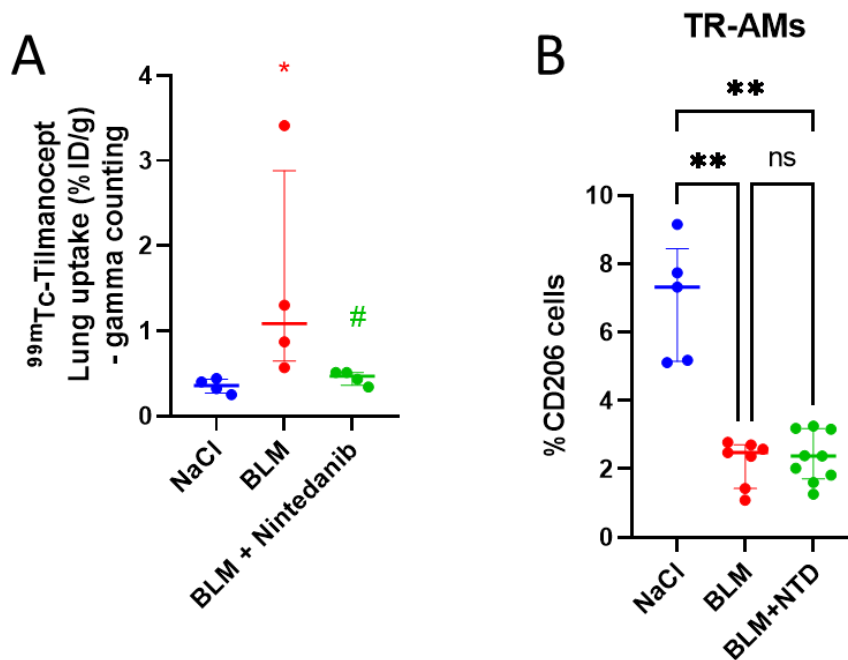


**Fig. S4**  $^{99m}\text{Tc}$ -tilmanocept is able to detect nintedanib efficacy

A/  $^{99m}\text{Tc}$ -tilmanocept lung uptake (%ID/g) at D23 by gamma counting of NaCl- and BLM-receiving mice treated or not with nintedanib. Results are presented as median  $\pm$  interquartile range, n = 4 for all groups. Stars (\*) are representative of comparison of each group with NaCl group and hashes (#) are representative of statistical comparison of BLM and BLM + nintedanib groups. Difference between groups were compared using Kruskal-Wallis non-parametric ANOVA. \*<sup>(#)</sup>p<0.05. B/ CD206 expression were expressed in percentage of cells expressing CD206 TR-AMs cells. Results are presented as median  $\pm$  interquartile range, NaCl n=5, BLM n=7, BLM+NTD n=9. Difference between groups were compared using Kruskal-Wallis non-parametric ANOVA. \*p<0.05, \*\*\*p<0.001.

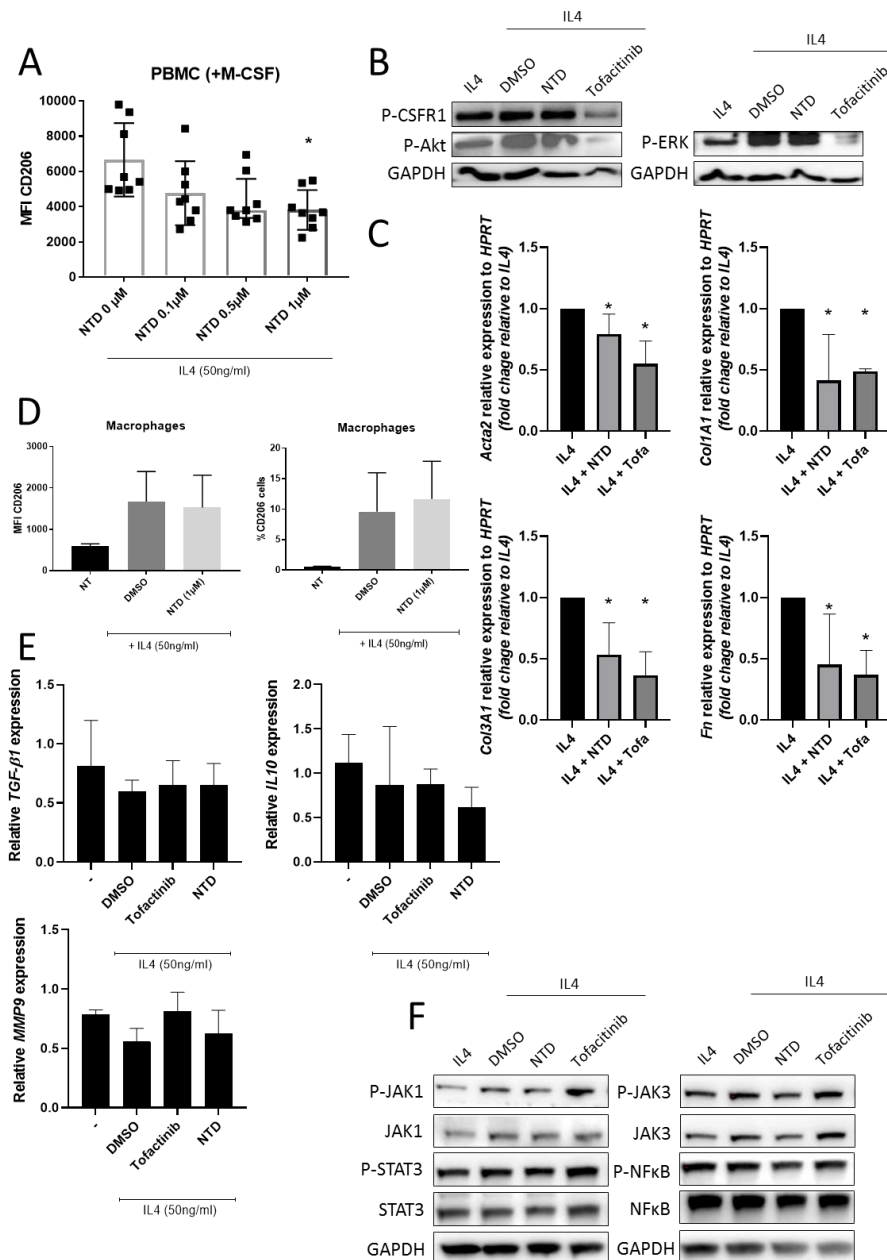


**Fig. S5 Nintedanib on CD206 macrophages in vitro**

A/ Macrophages isolated from healthy donor peripheral blood mononuclear cells (PBMC) were treated for 7 days with M-CSF (100ng/ml) and then incubated 48h with IL4 (50ng/ml) with or without NTD (0 $\mu$ M, 0.1 $\mu$ M, 0.5 $\mu$ M and 1 $\mu$ M). Results are presented as median  $\pm$  interquartile range from 8 independent experiments. Stars (\*) are representative of comparison of each group with NTD 0 $\mu$ M. Difference between groups were compared using Kruskal-Wallis non-parametric ANOVA. \* $p$ <0.05. B/ Macrophages isolated from healthy donor peripheral blood

mononuclear cells (PBMC) were treated for 7 days with M-CSF (100ng/ml) and then incubated 48h with IL4 (50ng/ml) with or without NTD or tofacitinib (1 $\mu$ M). Phosphorylation of CSFR1, AKT and ERK was monitored by immunoblotting. C/ CCD-19Lu human macrophages were treated 48h with conditioned media from macrophages isolated from healthy donor PBMC treated for 7 days with M-CSF (100ng/ml) and then incubated 48h with IL4 (50ng/ml) with or without NTD or tofacitinib (1 $\mu$ M). *Acta2*, *Col1A*, *Col3A1* and *Fn* expression was measured by RT-qPCR. Results are presented as median  $\pm$  interquartile range from 4 independent experiments. Stars (\*) are representative of comparison of each group with IL4 alone. Difference between groups were compared using Mann-Whitney non-parametric test. \* $p < 0.05$ . D/ CD206 expression analysis by flow cytometry after nintedanib treatment. The macrophages were first differentiated for 7 days by M-CSF and then treated by IL4 (50ng/ml) for 48h hours. Next, cells were treated by nintedanib (1 $\mu$ M) or DMSO (control, 1 $\mu$ M) for 48h hours. E/ Following to the treatments with nintedanib or tofacitinib, the expression of pro-fibrotic genes (TGF- $\beta$ 1, IL10 and MMP9) was assessed by RT-qPCR. F/ Macrophages isolated from healthy donor PBMC were treated for 7 days with M-CSF (100ng/ml) and then incubated 48h with IL4 (50ng/ml) and then incubated for extra 48h with or without NTD or tofacitinib (1 $\mu$ M). Phosphorylation of JAK1/3, STAT3 and NF $\kappa$ B was assessed by immunoblotting.

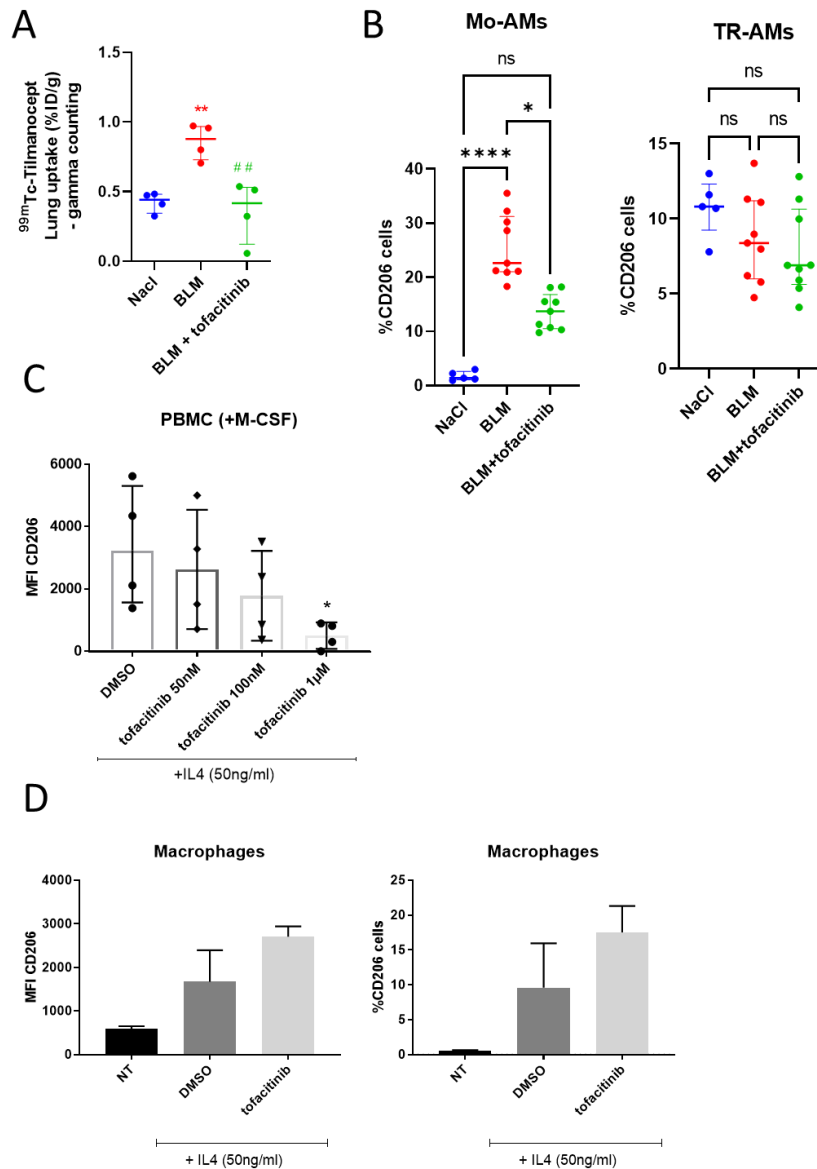


**Fig. S6**  $^{99m}\text{Tc}$ -tilmanocept is able to detect tofacitinib efficacy

A/  $^{99m}\text{Tc}$ -tilmanocept lung uptake (%ID/g) at D23 by gamma counting of NaCl- and BLM-receiving mice treated or not with tofacitinib. Results are presented as median  $\pm$  interquartile range,  $n = 4$  for all groups. Stars (\*) are representative of comparison of each group with NaCl group and hashes (#) are representative of statistical comparison of BLM and BLM + tofacitinib groups. Difference between groups were compared using Kruskal-Wallis non-parametric ANOVA. \*\*(##) $p < 0.01$ . B/ CD206 expression was expressed in percentage of cells expressing CD206 in Mo-AMs and TR-AMs cells. Results are presented as median  $\pm$  interquartile range, NaCl  $n = 5$ , BLM  $n = 7$ , BLM+NTD  $n = 9$ . Difference between groups were compared using Kruskal-Wallis non-parametric ANOVA. \* $p < 0.05$ , \*\*\* $p < 0.001$ . C/ Macrophages isolated from

healthy donor peripheral blood mononuclear cells (PBMC) were treated for 7 days with M-CSF (100ng/ml), and then incubated 48h with IL-4 with tofacitinib (50nM, 100nM, 1 $\mu$ M) or DMSO. Results are presented as median  $\pm$  interquartile range from 4 independent experiments. Stars (\*) are representative of comparison of each group with DMSO. Difference between groups were compared using Kruskal-Wallis non-parametric ANOVA. \*p<0.05. D/ CD206 expression analysis by flow cytometry after tofacitinib treatment. The macrophages were first differentiated for 7 days by M-CSF and then treated by IL4 (50ng/ml) for 48h hours. Next, cells were treated by tofacitinib (1 $\mu$ M) or DMSO (control, 1 $\mu$ M) for 48h hours.

Table 1	NaCl	BLM D8	BLM D15	BLM D22	Blocking
Number of values	12	6	6	15	12
Median	1,268	2,674 *	4,121 ***	3,697 ***	1,808 ###
Interquartile range	0,7504	0,855	3,206	2,235	0,712

**Table S1 <sup>99m</sup>Tc-tilmanocept is able to detect advanced bleomycin (BLM)-induced lung fibrosis-SPECT**

Values represent the <sup>99m</sup>Tc-tilmanocept lung uptake in %ID/g of NaCl- and BLM-receiving mice at D8, D15 and D22. Results are presented as median  $\pm$  interquartile range, NaCl n=12, BLM D8 n=6, BLM D15 n=6, BLM D22 n=15. Stars (\*) are representative of comparison of each group with NaCl group and hashes (#) are representative of statistical comparison of blocking group with BLM D22 group. Difference between groups were compared using Kruskal-Wallis non-parametric ANOVA, \*p<0.05, \*\*\*(###)p<0.001.

Table 2	NaCl	BLM D8	BLM D15	BLM D22	Blocking
Number of values	12	6	6	15	12
Median	-285,7	-181,8 *	-139,9 **	-137 ***	-142,6 **
Interquartile range	63,8	56,4	71,09	117,78	151,6

**Table S2 <sup>99m</sup>Tc-tilmanocept is able to detect advanced bleomycin (BLM)-induced lung fibrosis-CT**

Values represent the mean lung density quantified on CT images of NaCl- and BLM-receiving mice at D8, D15 and D22. Results are presented as median  $\pm$  interquartile range, NaCl n=12, BLM D8 n=6, BLM D15 n=6, BLM D22 n=15. Difference between groups were compared using Kruskal-Wallis non-parametric ANOVA. \*p<0.05, \*\*p<0.01, \*\*\*p<0.001.

Table 3	NaCl		BLM		BLM + nintedanib	
	Median	Interquartile range	Median	Interquartile range	Median	Interquartile range
D-1	1,2	0,3026	1,37	0,9625	1,075	0,8575
D9	1,07095	0,267025	2,745 *	1,52	2,87 *	1,1125
D16	1,28	0,54815	3,23 **	1,4175	1,68	0,8325
D23	1,225	0,23065	3,325 **	0,695	1,495 ###	0,57

**Table S3 In vivo imaging of CD206 is a useful tool to monitor nintedanib efficacy-SPECT**

Values represent evolution of <sup>99m</sup>Tc-tilmanocept lung uptake (%ID/g) at all time points. Results are presented as median  $\pm$  interquartile range, n = 4 for all groups. Stars (\*) are representative of statistical comparison between time points for each groups and hashes (#) are representative of statistical comparison between the groups at each time points. Difference between groups were compared using Kruskal-Wallis non-parametric ANOVA. \*p<0.05, \*\*(\*)p<0.01. Black arrow represents the start of treatments.

Table 4	NaCl		BLM		BLM + nintedanib	
	Median	Interquartile range	Median	Interquartile range	Median	Interquartile range
D-1	-292,82125	52,14305	-293,7412	33,32765	-284,7041	28,498425
D9	-292,629	51,086225	-189,9627 *	62,3881	-184,325835 *	45,3127175
D16	-281,8309	41,4303	-142,0504 **	87,1678875	-218,85455	39,9695
D23	-292,9709	51,2612	-166,13285 **	73,29905	-243,25195 ##	35,647325

**Table S4 In vivo imaging of CD206 is a useful tool to monitor nintedanib efficacy-CT**

Values represent evolution of mean lung densities (Mean CT density) of NaCl- and BLM-receiving mice treated or not with nintedanib at D0, D9, D16 and D23. Results are presented as median ± interquartile range, n = 4 for all groups. Stars (\*) are representative of statistical comparison between time points for each group and hashes (#) are representative of statistical comparison between the groups at each time point. Difference between groups were compared using Kruskal-Wallis non-parametric ANOVA. \*<sup>(#)</sup>p<0.05, \*\*p<0.01.

Table 5	NaCl		BLM		BLM + nintedanib	
	Median	Interquartile range	Median	Interquartile range	Median	Interquartile range
D-1	1,19	0,36585	1,62	0,1275	1,36	1,26
D9	0,9281	0,24905	2,545 **	1,2075	2,925 ***	2,1075
D16	1,113	0,1765	2,355 **	1,85	1,885	1,1075
D23	1,32935	0,519675	3,52 **	2,16	1,88 ####	0,5075

**Table S5 In vivo imaging of CD206 is a useful tool to monitor tofacitinib efficacy-SPECT**

Values represent evolution of <sup>99m</sup>Tc-tilmanocept lung uptake (%ID/g) at all time points. Results are presented as median ± interquartile range, n = 4 for all groups. Stars (\*) are representative of statistical comparison between time points for each group and hashes (#) are representative of statistical comparison between the groups at each time points. Difference between groups were compared using Kruskal-Wallis non-parametric ANOVA. \*\*p<0.01, \*\*\*(###)p<0.001.

Table 6	NaCl		BLM		BLM + nintedanib	
	Median	Interquartile range	Median	Interquartile range	Median	Interquartile range
D-1	-348,5852	98,89755	-316,92595	85,3862	-327,09615	78,321975
D9	-307,8591	84,1971	-246,717	117,81	-257,143	91,31125
D16	-313,70145	96,0161	-184,10565 ***	89,30805	-251,10185	66,3451
D23	-305,1962	40,2169	-186,13045 **	51,981725	-266,1228 #	57,0146

**Table S6 In vivo imaging of CD206 is a useful tool to monitor tofacitinib efficacy-CT**

Values represent evolution of mean lung densities of NaCl- and BLM-receiving mice treated or not with tofacitinib at D0, D9, D16 and D23. Results are presented as median ± interquartile range, n = 4 for all groups. Stars (\*) are representative of statistical comparison between time points for each group and hashes (#) are representative of statistical comparison between the groups at each time point. Difference between groups were compared using Kruskal-Wallis non-parametric ANOVA. #p<0.05, \*\*p<0.01, \*\*\*p<0.001.

## References

1. Savary, G., et al., *The Long Noncoding RNA DNMT3OS Is a Reservoir of FibromiRs with Major Functions in Lung Fibroblast Response to TGF-beta and Pulmonary Fibrosis*. Am J Respir Crit Care Med, 2019. **200**(2): p. 184-198.
2. Angelidis, I., et al., *An atlas of the aging lung mapped by single cell transcriptomics and deep tissue proteomics*. Nat Commun, 2019. **10**(1): p. 963.



3. Stoeckius, M., et al., *Cell Hashing with barcoded antibodies enables multiplexing and doublet detection for single cell genomics*. Genome Biol, 2018. **19**(1): p. 224.
4. Hao, Y., et al., *Integrated analysis of multimodal single-cell data*. Cell, 2021. **184**(13): p. 3573-3587 e29.
5. Joshi, N., et al., *A spatially restricted fibrotic niche in pulmonary fibrosis is sustained by M-CSF/M-CSFR signalling in monocyte-derived alveolar macrophages*. Eur Respir J, 2020. **55**(1).
6. Eversole, R.R., C.D. Mackenzie, and L.J. Beuving, *A photoreactive fluorescent marker for identifying eosinophils and their cytoplasmic granules in tissues*. J Histochem Cytochem, 2003. **51**(2): p. 253-7.